

## RELAXATION TIME OF POLYMER SOLUTIONS FROM ROD-CLIMBING HEIGHT (PART 2)

Hyoung Jin Choi\* and Hyoung Jae Kim

Department of Polymer Science and Engineering, Inha University, Inchon, Korea

(Received 15 November 1991 • accepted 1 May 1992)

**Abstract**—Relaxation time of the polymer solution from rod-climbing experiment is analyzed in this investigation. For a low deformation rate, the polymer solution can be regarded as a second-order fluid and rod-climbing constant for the second-order fluid is correlated with the rheological properties of that polymer solution. Climbing constant( $\beta$ ) of polymeric fluid is measured first and then from the correlation between rod-climbing constant and relaxation time of the polymer solution which we have obtained previously, the experimental relaxation time of PIB(polyisobutylene)-PB(polybutene)-kerosene system is obtained. In addition, by analyzing the molecular weight distribution of polymers, we also calculate the relaxation time based on the Muthukumar and Freed theory which was derived by generalizing the effective medium theory of the hydrodynamics of a polymer solution. Relaxation times from the rod-climbing experiment are found to be well correlated with the theoretical relaxation times.

### INTRODUCTION

It is well known that in a polymeric liquid, it climbs up the rod in contrast with the phenomenon which is held in a Newtonian fluid. The climb is associated with nonlinear effect and normal stress of the polymer solution, which cannot occur in fluids like Newtonian fluids, in which the stress is linearly related to the gradient of velocity.

Many researchers have scrutinized this rod-climbing phenomenon both theoretically and experimentally since Weissenberg [1] explained this effect from the normal stress concept of the polymer solution and added that the simple notation of an extra tension along the streamline could be used to obtain qualitative explanation of this phenomenon. The streamlines are closed circles and the extra tension along the lines strangulates the fluid and forces it inwards against the centrifugal force and upwards against the gravitational force in the rod-climbing experiment. Furthermore, from the physical nature of Rivlin's solutions, Serrin [2] obtained the same result as Weissenberg did for an incompressible Reiner-Rivlin fluid. In a Couette flow of an infinite cylinder, Coleman et al. [3] determined the direction of climbing using the value of the overthrust of the normal stress on a fictitious

plane of constant pressure along the axis. For the second-order fluids, the first analysis of rod-climbing was carried out by Giesekus [4], neglecting both inertia and surface tension.

Recently the most intensive works in this field have been carried out by Joseph and his research group [5-10]. Joseph and Fosdick [5] developed a systematic construction in series of the shape of the free surface above a simple fluid from the perturbation of a state of rest. The perturbation construction which they carried out gave a quantitative theory of climbing when the cylinder speeds were low. From the shape of the free surface, they determined the value of the climbing constant at the lowest-order deformation of a polymer solution. In their consecutive paper, Joseph et al. [6] observed the rod-climbing height in a vat filled with STP motor oil additive and mentioned that it was not possible to give a quantitative theory for the climbing observed in their experiments without accounting for the effects of surface tension. In addition, for the purpose of the development of practical methods of viscometry to characterize non-Newtonian fluids in slow flow, Beavers and Joseph [7] applied the measurements of the free surface near rods rotating in polymeric fluids and the theory of rod climbing to a viscometer for determining the values of certain constants that arise in the theory of slow flow using the method of slopes and the method of profile fitting.

\*To whom all correspondence should be addressed.

Since the shape of the free surface is very sensitive to changes in forces occurring at the surface, a free-surface rotating viscometer at low rates of shear uses the shape of the free surface as a barometer for measuring the distribution of stresses at the surface.

In this study, a brief derivation of the rod-climbing height is reviewed first and then as a continuation of the previous work by Choi [11], the result of rod-climbing experiment for the second-order fluid is being correlated with the rheological properties (the first and second normal stress difference coefficients) of the polymer solution. Thereafter from the correlation of the first normal stress difference coefficient and the relaxation time of polymer solution, the experimental relaxation time is finally calculated from the rod-climbing constant for polyisobutylene(PIB)-polybutene(PB)-kerosene system.

In addition, since our sample is highly polydisperse, the average relaxation times are calculated from the molecular weight distribution measured by gel permeation chromatography and the average relaxation times obtained theoretically from Muthukumar and Freed are compared with the relaxation times obtained from the rod-climbing experiment. Being compared with other experimental methods, it is found that the relaxation time from this method is rather simple to obtain.

## THEORETICAL BACKGROUNDS

### 1. The Climbing Constant

The climbing property of non-Newtonian fluids can be used to characterize important rheological parameters in those fluids. The most important of these is the climbing constant,  $\beta = 3\alpha_1 + 2\alpha_2$  where  $\alpha_1$  and  $\alpha_2$  are the parameters of the second-order approximation to the stress in a slowly varying flow of any simple non-Newtonian fluid. This climbing constant arises in the analysis of rod climbing, and is proportional to the height of climb in slow steady flow. It appears in some perturbation studies of Kaye [12], and Joseph and Fosdick [5]. On the other hand, Joseph et al. [6] showed that it is necessary to include surface tension effects if  $\beta$  is to be computed from measured values of the climb.

By a perturbation method, the shape of free surface is found to be expressed in the following form [5].

$$h(r, \omega) = h_s(r) + h_2(r)\omega^2 + O(|\omega^3|), \quad (1)$$

where  $\omega$  is the angular frequency of the rod and  $h_s(r)$  is the static climb. When surface tension is neglected,  $h_2(r)$  is also found to be represented as follows:

$$h_2(r) = \frac{4\pi^2}{\rho g} \left[ \frac{2a^4}{r^4} \beta - \frac{\rho a^4}{2r^2} \right] \quad (2)$$

where  $a$  is the radius of the rotating rod,  $\rho$  is the density of the liquid, and  $g$  is the gravity.

Eq. (2) could be used to compute  $\beta$  from measurements of  $h(r, \omega)$  for small  $\omega$ . Furthermore Joseph et al. [6] showed that to get the shapes of  $h(r, \omega)$  to agree with measured ones, it is necessary to retain the effects of surface tension.

In this case the height rise function  $h_2(r)$  is governed by the following equation:

$$\frac{\sigma}{r} (rh_2)' - \rho gh_2 = -\frac{2a^4}{r^4} \beta + \frac{\rho a^4}{2r^2} \quad (3)$$

$$h_2(a) = 0, \quad h_2(r) \rightarrow 0 \text{ as } r \rightarrow \infty$$

where  $\sigma$  is the surface tension.

Considering this surface tension, the two-parameter expansion procedure is adopted in Eq. (3) and then a very accurate approximate solution for the second-order was obtained by Joseph et al. [6]. When evaluated at the rod, this solution gives

$$h(a, \omega) \approx h_s(a) + \frac{4\pi^2 a}{\sigma \sqrt{S}} \left[ \frac{4\beta}{4 + \kappa} - \frac{\rho a^2}{2 + \kappa} \right] \frac{\omega^2}{2} \quad (4)$$

where  $\kappa = a(S)^{1/2}$  and  $S = \rho g / \sigma$ .

From the fact that the observed values of  $h$  vary linearly with  $\omega^2$  in the rod-climbing experiment,  $\beta$  is calculated with the known values of  $\sigma$  and  $(dh/d\omega^2)_{\omega=0} \rightarrow 0$  as follows:

$$\beta = \frac{4 + \kappa}{4} \left[ \frac{\sigma \sqrt{S}}{2\pi^2 a} \left( \frac{dh}{d\omega^2} \right)_{\omega=0} + \frac{\rho a^2}{2 + \kappa} \right]. \quad (5)$$

On the other hand, from the second-order fluid model, the rheological properties are obtained as a function of second-order parameters. The result of rod-climbing experiment which is combined with the coefficients of a second-order fluid model, is then correlated with the first ( $\Psi_1$ ) and second ( $\Psi_2$ ) normal stress difference coefficients as the following equation:

$$\beta = \Psi_1/2 + 2\Psi_2. \quad (6)$$

Furthermore, from the retarded motion expansion of the Zaremba-Fromm-Dewitt equation and the CEF constitutive equation, Choi [11] correlated the relaxation time of a polymer solution with the rod-climbing constant as follows:

$$\lambda = \frac{4 + \kappa}{4\eta} \left[ \frac{\sigma \sqrt{S}}{2\pi^2 a} \left( \frac{dh}{d\omega^2} \right)_{\omega=0} + \frac{\rho a^2}{2 + \kappa} \right]. \quad (7)$$

This was the first attempt to correlate the relaxation time with the rod-climbing experiment for the second-

order fluid. With the informations of a polymer solution such as density, surface tension and solution viscosity, the experimental relaxation time by simply measuring the free-surface from Eq. (1) could be obtained.

## 2. Theoretical Relaxation Time

Another relaxation time can be theoretically calculated from the molecular weight distribution of the polymer [13]. Muthukumar and Freed [14] derived the concentration dependent relaxation times by generalizing the effective medium theory of the hydrodynamics of a polymer solution and the relaxation time ( $\lambda_p$ ;  $p=1, 2, \dots, n$ ) is given as:

$$\lambda_p = \lambda_p'' (1 + ACp^{-1/2}) \quad (p=1, 2, \dots, n) \quad (8)$$

Here,

$$\lambda_p'' = \left( \frac{1}{96\pi} \right)^{1/2} \left( \frac{n!^2}{p} \right)^{3/2} \frac{\eta_s}{kT} \quad (9)$$

and

$$A = \left( \frac{\pi n}{24} \right)^{1/2} \frac{N_A l^3}{M_A} \quad (10)$$

where  $C$  is the polymer concentration in  $\text{g/cm}^3$ ;  $n$ ,  $l$ ,  $M_A$  are number, length and molecular weight of chain segments;  $\lambda_p$  is the relaxation time in sec;  $\lambda_p''$  is the relaxation time at infinite dilution;  $\eta_s$  is the solvent viscosity in poise;  $N_A$  is Avogadro's number;  $T$  is an absolute temperature in K, and  $k$  is the Boltzmann's constant. Eq. (9) depends on the molecular weight and the solvent viscosity, and Eq. (10) depends only on the molecular weight. Therefore, Eq. (8) shows that the longest relaxation time of a polymer chain is directly proportional to the solvent viscosity for any given polymer molecule.

The relaxation time from Eq. (8) can be simplified by putting  $M_A = 56 \text{ g/mol}$ ,  $l = 5.96 \times 10^{-8} \text{ cm}$  (from the end-to-end chain lengths of PIB) [15], and  $kT = 4.18 \times 10^{-14} \text{ gcm}^2 \text{ s}^{-1}$ . The only relaxation time which is relevant to our experiment is the longest one ( $p=1$ ), defined as  $\lambda_i$  (i.e.  $\lambda_i = \lambda_1$ ). The longest relaxation time for PIB, can be expressed as:

$$\lambda_i = 6.9185 \times 10^{-13} \eta_s M^{3/2} (1 + 9.565 \times 10^{-4} M^{1/2} C) \quad (\text{sec}) \quad (11)$$

where  $M$  is the molecular weight and  $C$  is the polymer concentration by weight percentage, and  $\eta_s$  is the solvent viscosity. Because our sample is highly polydisperse, we must also obtain the average relaxation time for the given molecular weight distribution. Eq. (11) was used to calculate the relaxation time in the molecular weight distribution curve with known values of

the polymer concentration and the solvent viscosity. The relaxation time for the each portion of the molecular weight spectrum from the GPC data. Three commonly used average of the relaxation times are defined as

$$\lambda_d = \frac{\sum_{i=1}^{\infty} \lambda_{(i)} N_i^{1+d}}{\sum_{i=1}^{\infty} N_i^{1-d}} \quad (12)$$

$d=0$ ; number average relaxation time ( $\lambda_n$ )

$d=1$ ; weight average relaxation time ( $\lambda_w$ )

$d=a$ ; viscosity average relaxation time ( $\lambda_v$ )

where  $\lambda_{(i)}$  is the relaxation time of molecular weight  $M_i$  as calculated from Eq. (12),  $N_i$  is the number of molecule of  $M_i$ .

## EXPERIMENTAL

### 1. Materials

High molecular weight PIB with different concentrations and different molecular weights in a mixed solvent of PB and kerosene were prepared for this rod-climbing experiment. The viscosity-average molecular weights of PIB (Vistanex; MM L-100, MM L-120 and MM L-140 which were obtained from Exxon Chemicals) were  $1.2 \times 10^6$ ,  $1.6 \times 10^6$  and  $2.1 \times 10^6 \text{ g/mol}$ , respectively.

Although PIB is compatible with PB, it is very difficult to dissolve without a co-solvent since Vistanex PIBs are highly paraffinic hydrocarbon polymers (its MM-grades are tough rubbery solids), composed of long straight-chain molecules having terminal unsaturation only with light colored, odorless, tasteless and nontoxic properties. Therefore small pieces of PIB were first dissolved in kerosene (Reagent Grade, Yakri Chemical Co.) using a magnetic stirring bar in a covered flask at room temperature for at least 24 hours. This solution of PIB in kerosene was then mixed into the PB with occasional stirring by hand, for at least one week. PB solvents (H-100 and H-300) were furnished by Amoco Chemical Company and those number-average molecular weights were 920 and 1290 g/mol, respectively.

The polymer solution was initially prepared as 0.3 %w/w and 0.5 %w/w solution in 7%w/w kerosene as a co-solvent and PB was then added. Complete dissolution occurred after allowing them to be homogeneous for one week.

### 2. Characterization of Polymers

The intrinsic viscosity of PIB was determined using a Ubbelohde suspended level type viscometer by

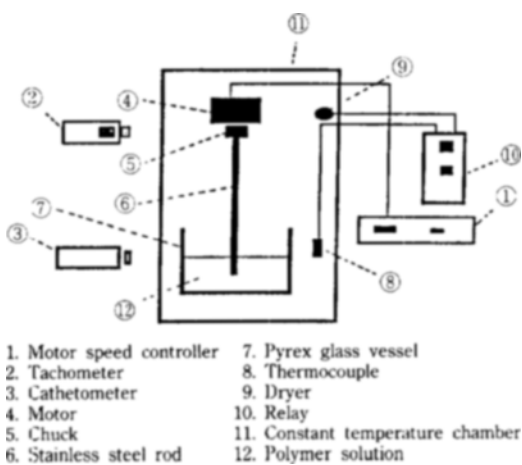


Fig. 1. Schematic diagram of rod-climbing experimental apparatus.

measuring the viscosity of the pure solvent and each of a series of dilute polymer solutions. 0.01 g/ml of PIB was first dissolved in toluene to make a stock solution, which was successively diluted with more toluene to obtain solutions of different polymer concentration. Finally, the Mark-Houwink-Sakurada equation,  $[\eta] = KM_r^a$ , with  $K = 1.25$  and  $a = 0.78$  at  $30.0^\circ\text{C}$  [12], was used to convert the measured intrinsic viscosity into the viscosity-averaged molecular weight  $M_v$ .

In addition, gel permeation chromatography(GPC) was also used to determine the distribution of molecular weights of each of the PIB samples. PIB was dissolved in tetrahydrofuran(GPC grade) to a concentration of 0.002 g/ml and analyzed by a Waters Model 510 GPC, equipped with a Waters 410 differential refractometer having a sample volume of  $20 \mu\text{l}$ . The packing material of a 4 ft long column was Ultrastyragel 500 A, and GPC was run at  $30^\circ\text{C}$  with tetrahydrofuran as the mobile phase. To analyze the GPC data, the universal calibration curve for polystyrene(the standard narrow fraction) was used [13].

On the other hand, using Cannon Fenske Routine Type capillary viscometers, the solution viscosities of PIB-PB-kerosene systems were also measured.

### 3. Rod-Climbing Apparatus

The rod-climbing experimental apparatus consists (Fig. 1) of centerless ground stainless steel rod of dimension 1.0 cm in diameter  $\times$  27.5 cm in length, enclosed in a thermostatically controlled container, which is made of Acrylate-Acetate(PMMA) and has a dimension of 25 cm  $\times$  45 cm  $\times$  80 cm. This system can maintain the chamber temperature to within  $\pm 0.2^\circ\text{C}$ . The essential part of this apparatus is a circular rod, which

is free to rotate about a vertical axis immersed in a large vat of fluid. To study the effect of rod size on the rod-climbing constant, two other different rods of 1.0 cm and 1.2 cm in diameter were used. The rod was driven from above by an Electrocraft DC servomotor with a control system [Sun Mi Technology Co. SMS20] to maintain constant speed under varying torque conditions. The motor and the rod were connected by a chuck. As mentioned by Beavers and Joseph [7], Scotch-Gard (commercial name) was coated for both vessel and rod to establish a 90 degree contact angle between the fluid and the rod, and also between the fluid and the vessel.

The apparatus can accommodate rods of any diameter up to approximately 1.2 cm. This limitation is imposed by the diameter of the fluid container(11 cm) with the requirement that the ratio of the container diameter to the rod diameter be greater than about 10 for the infinite fluid approximation to be valid.

The angular speed of the rod was measured by means of a digital tachometer [Lutron Co. DT-2234A] with an accuracy of 0.5 rpm and fixed at constant angular speed for each experiment. The height of climb of the fluid was then measured with the aid of a cathetometer [Gaertner Scientific Corporation M 940-300P]. Measurements are repeatable to within 0.001 mm.

### 4. Measurement of $\beta$

The value of  $\beta$  is determined from the measured values of the height of climb on the rod. The rod is rotated slowly, at a speed for which a measurable height of climb can just be distinguished. The climb is measured as a function of increasing rotational speed, and the slope of  $h(r, \omega)_{r=a}$  versus  $\omega^2$  is computed for  $\omega \rightarrow 0$ ,

$$h_2(a) = \frac{dh(r, \omega)}{d\omega^2} \Big|_{r=a} \omega \rightarrow 0, \quad (13)$$

and the measured value of the slope was inserted into Eq. (5) to determine  $\beta$ . Therefore, from Eqs. (6) and (7), the relaxation time of the polymer solution is finally obtained from the rod-climbing experiment.

## RESULTS AND DISCUSSION

Most of the works on the rod-climbing in this investigation are emphasized on the polymer solution properties, such as polymer concentration, different molecular weight, and mixed solvent system.

Figs. 2 and 3 show the shear rate dependence of the shear stress and shear viscosity of the test liquids using a Carri-Med Rheometer system. It is found that

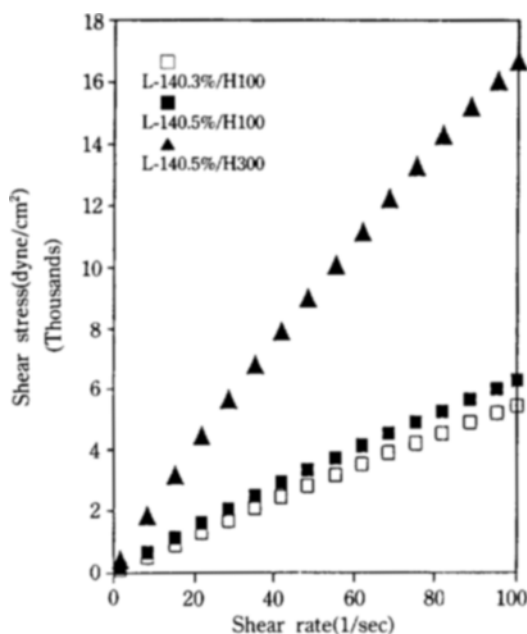


Fig. 2. Shear stresses of PIB-PB-Kerosene solutions as functions of shear rate. All stresses was measured with the cone and plate rheometer at 30°C.

PIB-PB-Kerosene system shows second-order fluid behavior with constant, high viscosity and high elasticity at room temperature even though there exists slight shear thinning behavior for 0.5% PIB(L-140) in H-300 PB and kerosene system. This fluid is often called "Boger fluid" [16]. However, PB-kerosene solvent shows Newtonian behavior with constant viscosity (Fig. 3).

On the other hand, in this experiment, because of some experimental errors, we do not measure elastic properties of the polymer solutions such as first normal stress difference and elastic modulus from dynam-

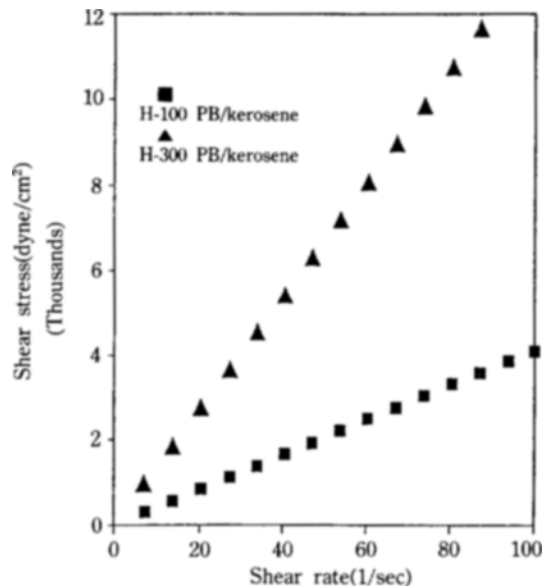


Fig. 3. Shear stress of solvent of solutions (H-100 PB/Kerosene and H-300 PB/Kerosene) as a function of shear rate.

ic test. However, for the similar systems with ours, elastic data are available in recent literatures [17-22]. Boger et al. [17, 18] measured first normal stress difference and storage modulus( $G'$ ) of PIB-PB-kerosene system and found that of all the highly elastic constant viscosity fluid available, that system is the most attractive. In addition, Quinzani et al. [19] also presented a detailed rheological study of PIB-PB-tetradecane(C 14).

The values of the climbing constants and  $\beta$  for solutions of Vistanex PIB in PB-Kerosene solvent are presented in Table 1. The rod-climbing constants( $\beta$ ) of each molecular weight increase with polymer concen-

Table 1. Summary of the rod-climbing data and the relaxation times for PIB-PB-kerosene systems

PIB	PIB content [% w/w]	$\eta_s$ [poise]	$(dh/d\omega^2)\omega \rightarrow 0$ [cm $\cdot$ sec $^2$ ]	$\beta$ [g/cm]	$\lambda_E$ (s) [sec]	$\lambda_\lambda$ (s) [sec]
Different molecular weight						
L-100	0.5	74.5	0.245	6.82	0.092	0.132
L-120	0.5	79.8	0.271	7.54	0.094	0.066
L-140	0.5	86.0	0.361	10.02	0.116	0.267
Different PIB concentration						
L-140	0.3	62.3	0.160	4.48	0.072	0.197
L-140	0.5	86.0	0.361	10.02	0.116	0.267
Different solvent viscosity						
L-140	0.5	86.0	0.361	10.02	0.116	0.267
L-140	0.5	229	2.110	61.89	0.271	0.904

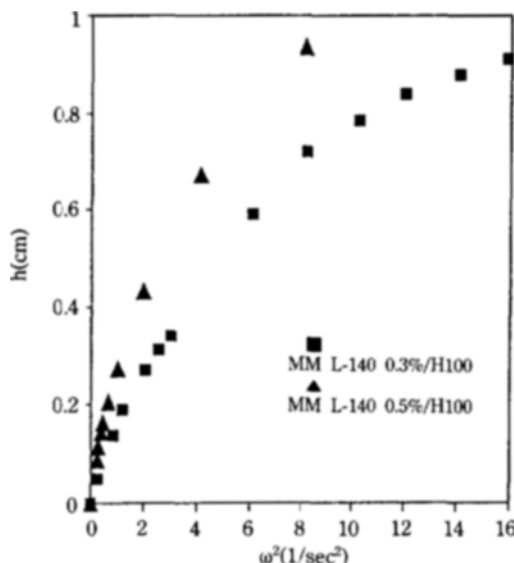


Fig. 4. Effect of polymer concentration(MM L-140 in H-100 PB-Kerosene solvent) on the rod-climbing height using a 1.0 cm diameter rod at 30°C.

tration, molecular weight and solvent viscosity.

### 1. Effect of PIB Concentration

Fig. 4 shows the rod-climbing height versus square of the rotation speed of the rod for two different concentrations of MM L-140 PIB in H-100 PB-Kerosene solvent. The higher concentration (high elasticity) results in the higher rod-climbing height.

In addition, the concentration effect on  $\beta$  can be considered from the theory developed by Brunn [23], who adopted Brinkman's analysis for the dumbbell model polymer in a second-order fluid and then obtained the following equations;

$$\eta = \eta_s(1 + C[\eta] + 0.5(C[\eta])^2)$$

$$\Psi_1 = \frac{2M\eta_s^2[\eta]^2C}{RT} (1 + 1.25 C[\eta])$$

$$\Psi_2 = \frac{-0.25 M\eta_s[\eta]^3C^2}{RT} \quad (14)$$

Inserting these equations into Eq. (6), we can find that the rod-climbing height is increased with increasing polymer concentration and solvent viscosity as the following equation;

$$\beta \propto \eta_s^2[\eta]^2C(1 + 0.75C[\eta]) \quad (15)$$

### 2. Effect of Solvent Viscosity

Fig. 5 shows that the rod-climbing height increases with solvent viscosity for 0.5% w/w PIB MM L-140 in two different solvent systems and correlates well

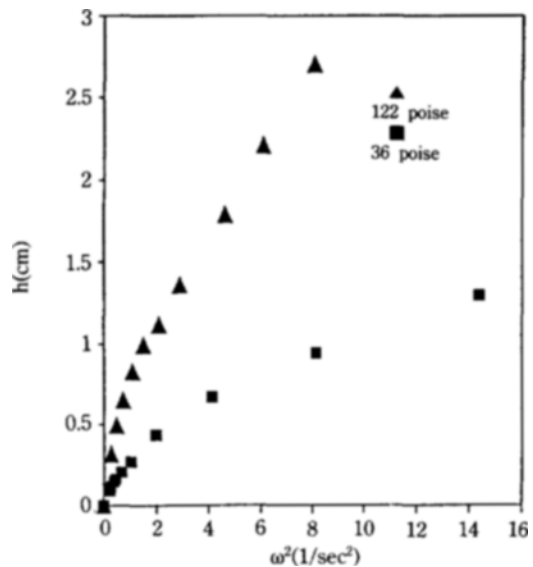


Fig. 5. Effect of solvent viscosity(MM L-140 0.5% w/w in two different PB-Kerosene solvent) on the rod-climbing height using a 1.0 cm diameter rod at 30°C.

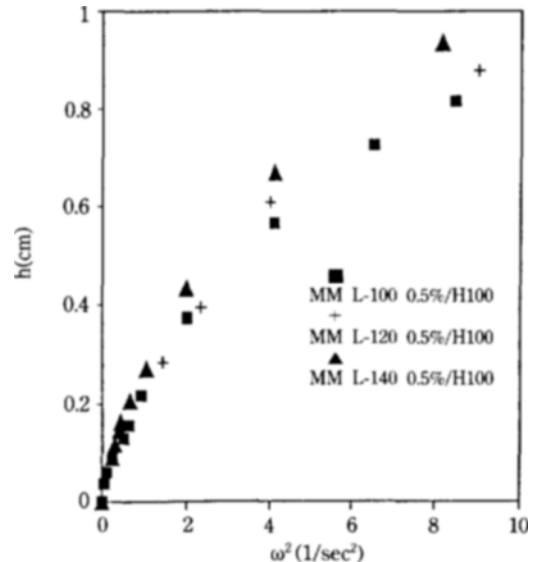


Fig. 6. Effect of polymer molecular weight(MM L-100 0.5% w/w, MM L-120 0.5% w/w and MM L-140 0.5% w/w in H-100 PB-Kerosene solvent) on the rod-climbing height using a 1.0 cm diameter rod at 30°C.

with the fact that  $\beta$  is proportional to the square of the solvent viscosity as shown in the above Eq. (15). Solvent viscosities of H-100 and H-300 were 36 poise

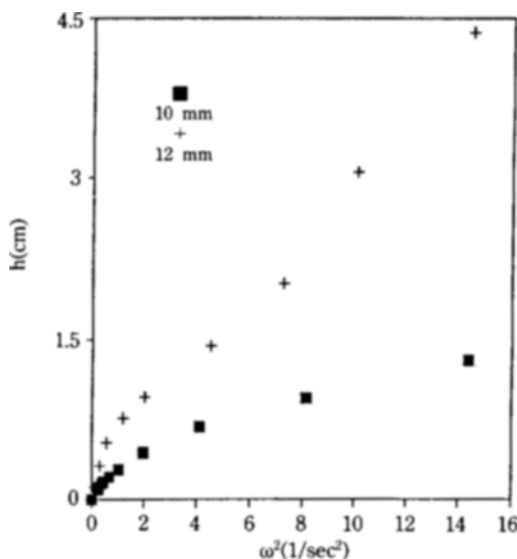


Fig. 7. Effect of Rod size (with 10 mm and 12 mm diameter rod) on the rod-climbing height for a MM L-140 0.5% w/w in H-300 PB-Kerosene solvent at 35°C.

and 122 poise.

### 3. Effect of Molecular Weight

The rod-climbing experiment was also performed for different PIB molecular weights in PIB-PB-Kerosene system. For 0.5% w/w of three different molecular weight samples of Vistanex PIB (MM L-100, MM L-120 and MM L-140) in PB-Kerosene solvent, there is an increase in the climbing constant with increase in molecular weight (Fig. 6).

### 4. Effect of Rod Size

Fig. 7 shows the rod-climbing height with respect to the square of the rotation speed of the rod with two different rod size for 0.5% w/w MM L-140 PIB in H-300 PB. The rod-climbing height increases with rotation speed and rod size as expected. Since  $\beta$  is almost identical for different rod sizes (smaller than  $R_c$ ), it is possible to choose any of the true rod sizes for use in the experiment. The 1.0 cm of rod size was chosen for convenience. For this effect of rod size, Joseph et al. [6] showed that the free surface rises only if  $r^2 < 4\beta/\rho$  when  $\omega$  is small. This result can be easily obtained from the fact that to get the rod-climbing, the right hand side of Eq. (2) should be positive. This relation provides the criteria of selecting the rod size and explains why it is better to use small diameter rods in the rod-climbing experiments. On the other hand, comparing Doi and Edwards model with Curtiss and Bird model, Hassager [24] argued that the Doi-

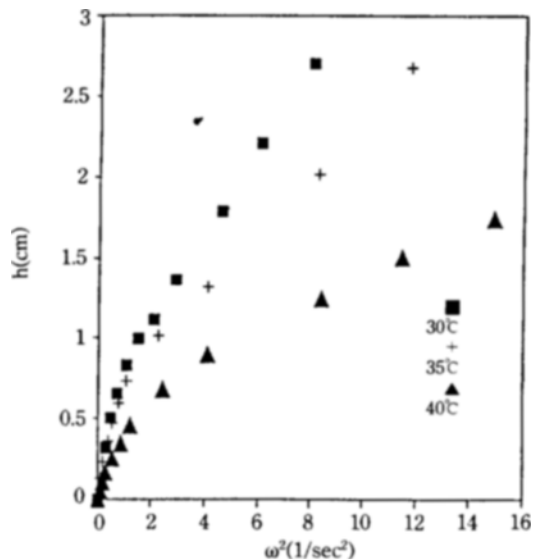


Fig. 8. Effect of experimental temperature (at 30°C, 35°C and 40°C) on the rod-climbing height for a MM L-140 0.5% w/w in H-300 PB-Kerosene solvent using a 1.0 cm diameter rod.

Edwards model will always predict "rod dipping", whereas the Curtiss-Bird model capable of predicting the experimentally observed rod-climbing when an additional parameter  $\varepsilon > 1/8$ . The monodisperse theory of Curtiss and Bird [25] gives the following correlation:

$$\Psi_2 = -\frac{2}{7}(1-\varepsilon)\Psi_1 \quad (16)$$

where  $\varepsilon$  is an additional parameter.

Therefore from Eqs. (6) and (16), the climbing constant is seen to be quite sensitive to the values of  $\varepsilon$  as follows;

$$\beta = \frac{1}{14}(8\varepsilon - 1)\Psi_1 \quad (17)$$

Therefore Curtiss-Bird theory with  $\varepsilon > 1/8$  predicts rod-climbing provided the radius of the rod is sufficiently small that inertia does not dominate.

However, Marrucci and Grizzuti [26] later investigated that if the independent alignment in the constitutive equation from Doi and Edwards [27, 28] is disregarded, their model correctly predicts a positive Weissenberg effect for slow flows.

### 5. Effect of Temperature and Surface Tension

For the temperature effect on the rod-climbing experiment, Beavers and Joseph [7] showed that the height of climb, which has a bell-shaped profile at the

rod, is largely influenced by the temperature of the fluid. They also showed that as the rotational speed is increased to very high values, the rod-climbing height decreases and is eventually replaced with an inertia-dominated depression of the free surface. This depression of the free surface at high speeds may be caused by viscous heating near the rod. Small changes in temperature may cause recognizable changes in the value of  $\beta$ . For example, they found that for STP

$$\beta = 20 \exp(-0.115T) \text{ gcm}^{-1}, \quad 25 < T(\text{°C}) < 50 \quad (18)$$

which is probably the only known empirical formula relating the temperature dependence to  $\beta$ . In our experiment, sufficient attention was paid to controlling the temperature. The temperature of the fluid was maintained at 30.0°C, in a water bath, with a  $\pm 0.2^\circ\text{C}$  error range.

Fig. 8 shows the effect of experiment temperature on the rod-climbing height with a 0.5%w/w MM L-140 PIB in H-300 PB-kerosene solvent. As predicted in Eq. (18), the rod-climbing height decreases as increasing the temperature.

On the other hand, it is found that the values of  $\sigma$  which have been measured in different liquids used in this experiment reported here are nearly the same [13]. Therefore, to find the effect of surface tension on the rod-climbing constant, the following argument is considered [29]. Under the conditions of most of the experiments, the second term on the right-hand side of Eq. (5) is small compared with the first and hence it gives

$$\beta = \left( \frac{4 + \kappa}{4} \right) \frac{\sigma \sqrt{S}}{2\pi^2 a} \left( \frac{dh}{d\omega^2} \right) \omega \rightarrow 0 \quad (19)$$

Thus, for fixed values of  $(dh/d\omega^2)$ ,  $\omega \rightarrow 0$ ,  $a$  and  $\rho$ , we have

$$\frac{d\beta}{\beta} = \left( \frac{2}{4 + \kappa} \right) \frac{d\sigma}{\sigma} \quad (20)$$

For the operating condition of our experiments ( $a = 0.5 \text{ cm}$ ,  $\rho = 0.87 \text{ g/cm}^3$ ,  $\sigma = 32.5 \text{ dyne/cm}$ ), Eq. (20) gives the following result

$$\frac{d\beta}{\beta} = 0.32 \frac{d\sigma}{\sigma} \quad (21)$$

So an error in the value of  $\sigma$  of 1% leads to an error in the computed value for  $\beta$  of about 0.32%. Therefore, it can be concluded that the value computed for  $\beta$  from the graph of the measured height of climb at the rod is not strongly affected by the small change in surface tension.

## 6. Relaxation Time of Polymer Solution

The relaxation times of the polymer solutions are calculated from the rod-climbing experiment in this investigation. With the known values of the density, solution viscosity, surface tension and the rod-climbing constant, the relaxation times are obtained from Eq. (7) and given in Table 1. In addition, Eq. (11) is used to calculate the relaxation times in the molecular weight distribution curve with known values of the polymer concentration and the solvent viscosity. The relaxation time for each portion of the molecular weight is calculated and summed for the molecular weight spectrum.

There are several reasons why the experimental relaxation time is different from the number-average relaxation time. First of all, there is an uncertainty associated with the relaxation time from the rod-climbing experiment. Since the second-order fluid model was used, the higher order terms were neglected and from the experimental point of view, the error also comes from the uncertainty of determining the slope when the square of the rotation speed goes to zero. On the other hand, deriving the theory in Section 2, we also assume that the second normal stress difference is zero. In addition, even though the kerosene system is a better solvent system rather than theta-solvent, theoretical relaxation time is based on the Muthukumar and Freed theory which assumes a theta-solvent. However, in spite of the difference between two relaxation times, the rod-climbing experiment can be regarded as a possible method to determine the relaxation time of polymer solutions.

## CONCLUSIONS

Rod-climbing constants and relaxation times of PIB-PB-kerosene system are investigated in this study. From the correlation between rod-climbing constant and relaxation time of the polymer solution, the experimental relaxation time of the polymer solution is obtained and then compared with the theoretical relaxation time.

The rod-climbing constants are also found to be increased with rod size, polymer concentration, solvent viscosity and molecular weight of polymer and it decreases with temperature. However, surface tension does not affect much on it.

## ACKNOWLEDGEMENT

The financial support from the Non Directed Research Fund of Korea Research Foundation is grate-

fully acknowledged.

## NOMENCLATURE

$a$	: rod radius
$g$	: gravity constant
$h$	: rod-climbing height
$h_s$	: static rise
$h_2$	: rod climbing height in Eq. (1)
$C$	: polymer concentration
$p$	: integer in Eq. (8)
$n$	: number of chain segments
$l$	: length of chain segments
$M_A$	: molecular weight of chain segments
$M$	: molecular weight
$k$	: Boltzmann constant
$T$	: temperature
$S$	: $\rho g / \sigma$

## Greek Letters

$\alpha_1, \alpha_2$	: second-order fluid constants
$\beta$	: rod-climbing constant
$\rho$	: fluid density
$\eta$	: solution viscosity
$\lambda$	: relaxation time
$\omega$	: rotation rate
$\sigma$	: surface tension
$\Psi_1$	: first normal stress difference coefficient
$\Psi_2$	: second normal stress difference coefficient
$\kappa$	: $a(s)^{1/2}$
$\eta_s$	: solvent viscosity
$[\eta]$	: intrinsic viscosity
$\lambda_\phi$	: relaxation time of $\rho$ mode

## REFERENCES

1. Weissenberg, K.: *Nature*, **159**, 310 (1947).
2. Serrin, J.: *Z. Angew. Math. Mech.*, **39**, 295 (1959).
3. Coleman, B. D., Markovitz, H. and Noll, W.: "Viscometric Flows of non-Newtonian Fluids", Springer Tracts in Natural Philosophy, Vol. 5, Springer-Verlag, Berlin, Germany (1966).
4. Giesekus, H.: *Rheol. Acta*, **1**, 403 (1961).
5. Joseph, D. D. and Fosdick, R. L.: *Arch. Rat. Mech. Anal.*, **49**, 321 (1973).
6. Joseph, D. D., Beavers, G. S. and Fosdick, R. L.: *Arch. Rat. Mech. Anal.*, **49**, 381 (1973).
7. Beavers, G. S. and Joseph, D. D.: *J. Fluid Mech.*, **69**(3), 475 (1975).
8. Beavers, G. S. and Joseph, D. D.: *J. Fluid Mech.*, **81**(2), 265 (1977).
9. Joseph, D. D. and Beavers, G. S.: *Rheol. Acta*, **16**, 169 (1977).
10. Joseph, D. D. and Beavers, G. S.: *Arch. Rat. Mech. Anal.*, **62**, 323 (1977).
11. Choi, H. J.: *Korean J. Chem. Eng.*, **8**(1), 18 (1991).
12. Kaye, A.: *Rheol. Acta*, **12**, 206 (1973).
13. Choi, H. J.: Ph.D. Dissertation, Carnegie Mellon University, Pittsburgh, PA (1987).
14. Muthukumar, M. and Freed, K. F.: *Macromolecules*, **11**, 843 (1978).
15. Flory, P. J.: "Principles of Polymer Chemistry", 8th ed., Cornell University Press, Ithaca, New York (1971).
16. Boger, D. and Nguyen, H.: *Polym. Eng. Sci.*, **18**, 1037 (1978).
17. Binnington, R. J. and Boger, D. V.: *Polym. Eng. Sci.*, **26**(2), 133 (1986).
18. Mackay, M. E. and Boger, D. V.: *J. Non-Newtonian Fluid Mech.*, **22**, 235 (1987).
19. Quinzani, L. M., McKinley, G. H., Brown, R. A. and Armstrong, R. C.: *J. Rheol.*, **34**(5), 705 (1990).
20. Prilutski, G., Gupta, R. K., Sridhar, T. and Ryan, M. E.: *J. Non-Newtonian Fluid Mech.*, **12**, 233 (1983).
21. Choplin, L., Carreau, P. J. and Ait Kadi, A.: *Polym. Eng. Sci.*, **23**(8), 459 (1983).
22. Choplin, L. and Carreau, P. J.: *Rheol. Acta*, **25**, 95 (1986).
23. Brunn, P.: *J. Rheol.*, **24**, 263 (1980).
24. Hassager, O.: *J. Rheol.*, **29**, 361 (1985).
25. Curtiss, C. F. and Bird, R. B.: *J. Chem. Phys.*, **74**, 2016 (1981)/**74**, 2026 (1981).
26. Marrucci, G. and Grizzuti, N.: *J. Non-Newtonian Fluid Mech.*, **21**, 319 (1986).
27. Doi, M. and Edwards, S. F.: *J. Chem. Soc. Farad. Trans. 2*, **74**, 1818 (1978).
28. Doi, M. and Edwards, S. F.: *J. Chem. Soc. Farad. Trans. 2*, **75**, 32 (1979).
29. Joseph, D. D., Beavers, G. S., Dewald, C., Hoger, A. and Than, P. T.: *J. Rheol.*, **28**, 325 (1984).